saturated, so no spectrum can be observed. At 5 K a rapid passage experiment with low microwave power demonstrates spin flipping for both complexes. To our knowledge this behavior has not been previously observed for mixed-valence species. At 350 K the ESR spectrum of V_2 consists of the expected 15 lines ($a = 51$ G) for a rapidly hopping electron interacting with two equivalent vanadium nuclei.[11] The corresponding spectrum of HV_3 is much more complex with more than 33 lines. We provisionally ascribe this to the lower symmetry of the protonated V_3O_{13} group which results in unequal interactions of the unpaired electron with the three vanadium nuclei.

Acknowledgment. We thank Dr. Hideo Kon, National Institute for Arthritis and Metabolic Diseases, and Dr. George Yang, Food and Drug Administration, for generously making spectrometers available for some of the ESR measurements and for advice. This research has been supported in part by NSF Grant No. CHE76-19571.

---

[11] Fifteen- and twenty-two-line spectra per se do not permit us to distinguish unequivocally between rapid electron hopping and electron delocalization (or indeed any combination of these). In the present case we conclude that electron hopping is the predominant mechanism leading to the observed "high-temperature" (300–400 K) spectra because the transition to the "trapped" eight-line spectrum occurs over a temperature range in which the samples are frozen aqueous glycerol glasses (thus ruling out the possibility that slight distortions induced by freezing render the three vanadiums of V_3 inequivalent). We can also show, by observation of unchanged IT spectra of HV_3 in benzene, dimethylformamide, and dimethyl sulfoxide, that the electron "trap" is almost entirely caused by intramolecular polarization and that effects of solvent polarization are negligible.

Bimetallic Catalysts from Pseudotetrahedral Iridium–Tungsten Clusters. Syntheses and Crystal Structures of $(\eta^5\text{-}C_5H_5)WIr_3(CO)_{11}$ and $(\eta^5\text{-}C_5H_5)_2W_2Ir_2(CO)_{10}$

John R. Shapley,* Steven J. Hardwick, Daniel S. Foose, and
Galen D. Stucky*[‡]

Department of Chemistry and
Materials Research Laboratory
University of Illinois, Urbana, Illinois 61801

Melvyn Rowen Churchill,* Clifford Bueno, and
John P. Hutchinson

Department of Chemistry
State University of New York at Buffalo
Buffalo, New York 14214

Received May 4, 1981

Sinfelt and co-workers[1] have pioneered the development and study of heterogeneous "bimetallic cluster" catalysts, i.e., materials composed of very small bimetallic particles highly dispersed over the surface of an oxide support. These materials customarily have been prepared by simultaneous or sequential impregnation of a separate precursor for each metal, which allows only gross control of stoichiometry. In principle, control of individual particle composition is possible by using appropriate precursor compounds containing both metals, e.g., a bimetallic cluster compound.[2] A critical test of this approach is to compare catalysts derived from two isostructural clusters $[(ML_n)_x(M'L'_m)_y]$, which have a different M/M′ ratio (x/y). Significant effects have been seen for the pair $Co_3Rh(CO)_{12}$ and $Co_2Rh_2(CO)_{12}$ as precursors,[3,4] but combinations of less similar transition metals[5] have not been examined. In part this may have been due to the lack of suitable compounds.[6] We now report the convenient syntheses and molecular structures of two tetranuclear iridium–tungsten clusters, $CpWIr_3(CO)_{11}$ (**1**) ($Cp \equiv \eta^5\text{-}C_5H_5$) and $Cp_2W_2Ir_2(CO)_{10}$ (**2**), together with their use as precursors to alumina-supported bimetallic catalysts.

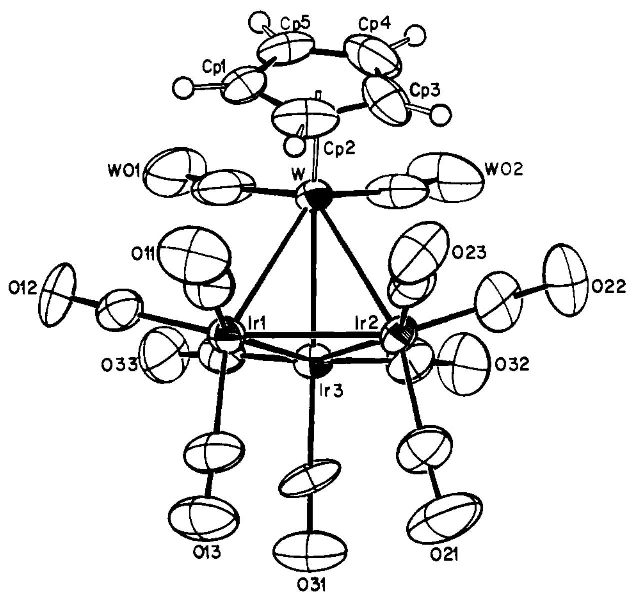

Figure 1. ORTEP diagram of the molecular structure of $CpWIr_3(CO)_{11}$ (**1**). Metal–metal distances within this molecule are Ir(1)–Ir(2) = 2.699 (1), Ir(1)–Ir(3) = 2.702 (1), and Ir(2)–Ir(3) = 2.697 (1) Å [average Ir–Ir = 2.699 (2) Å, compared with 2.693 Å in $Ir_4(CO)_{12}$; W–Ir(1) = 2.815 (1), W–Ir(2) = 2.792 (1), and W–Ir(3) = 2.865 (1) Å (average W–Ir = 2.824 (37) Å].

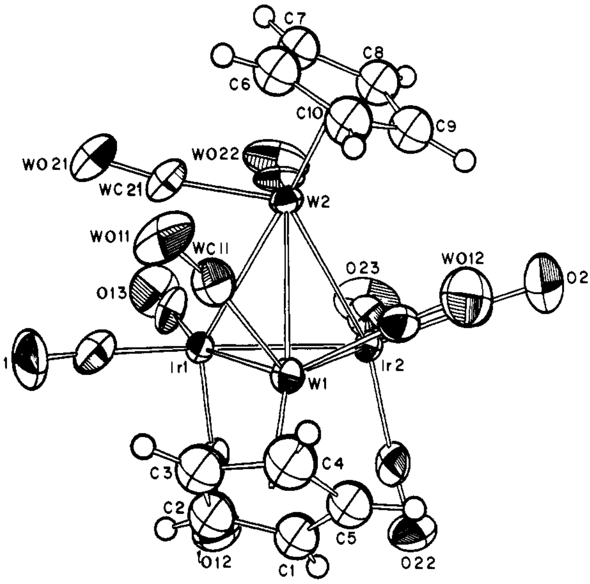

Figure 2. ORTEP diagram of the molecular structure of $Cp_2W_2Ir_2(CO)_{10}$ (**2**). Metal–metal distances within the molecule are W(1)–W(2) = 2.991 (1), Ir(1)–Ir(2) = 2.72 (1), W(1)–Ir(1) = 2.796 (1), W(1)–Ir(2) = 2.833 (1), W(2)–Ir(1) = 2.863 (1), and W(2)–Ir(2) = 2.847 (1) Å (average W(1)–Ir = 2.815, average W(2)–Ir = 2.855 Å).

The combination of $IrCl(CO)_2NH_2C_6H_4Me$ and excess $CpW(CO)_3H$ (CH_2Cl_2, 60 °C, 6 h, 40 psig of CO) in the presence of

---

[‡] Central Research and Development Department, Experimental Station, E. I. du Pont de Nemours and Co., Wilmington, DE 19898.

[1] Sinfelt, J. H. *Acc. Chem. Res.* **1977**, *10*, 15 and references therein. Sinfelt, J. H.; Via, G. H. *J. Catal.* **1979**, *56*, 1 and references therein.

[2] Anderson, J. R.; Mainwaring, D. E. *J. Catal.* **1974**, *35*, 162.

[3] (a) Anderson, J. R.; Elmes, P. S.; Howe, R. F.; Mainwaring, D. E. *J. Catal.* **1977**, *50*, 508. (b) Anderson, J. R.; Mainwaring, D. E. *Ind. Eng. Chem. Prod. Res. Dev.* **1978**, *17*, 202.

[4] Ichikawa, M. *J. Catal.* **1979**, *59*, 67.

[5] For the novel use of *potassium* carbonyl ferrates as precursors to Fischer–Tropsch catalysts, see: McVicker, G. B.; Vannice, M. A. *J. Catal.* **1980**, *63*, 25. See also ref 32.

[6] Review of mixed-metal clusters: Gladfelter, W. L.; Geoffroy, G. L. *Adv. Organometal. Chem.* **1980**, *18*, 207.

0002-7863/81/1503-7383$01.25/0

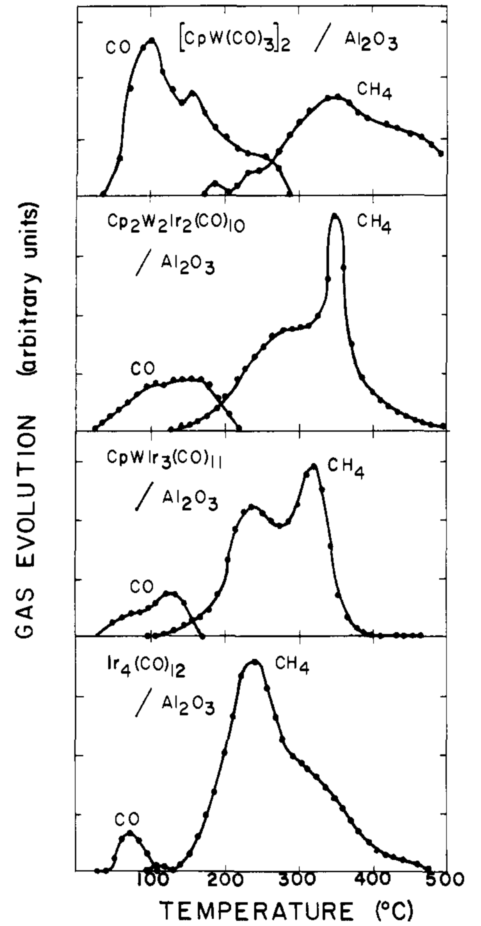

Figure 3. Profiles for carbon monoxide and methane evolution during the temperature programmed decomposition of alumina-supported carbonyl compounds in flowing H_2. The heating rate was 3.9 °C/min and the H_2 flow rate was 20 mL/min. The samples contained 3–5 mg of compound on 0.5 g of alumina.

zinc provided after TLC red $[CpW(CO)_3]_2$, orange **1**[7] (70–80%), and brown **2**[8] (trace). A high yield of **2** (85%) was obtained from the reaction of $IrCl(CO)_2NH_2C_6H_4Me$ and excess $Na[CpW(CO)_3](CH_2Cl_2$, 25 °C, 2 h). Compounds **1** and **2** were not interconvertible at room temperature, but after treatment of **2** with CO at 110 °C (C_6H_{12}, 40 psig, 2 h) 53% of **1** was recovered.

The molecular structures of **1**[9] (see Figure 1) and **2**[10] (see Figure 2) are analogous to that of $Ir_4(CO)_{12}$[12] but with one and two $Ir(CO)_3$ units, respectively, replaced by isoelectronic $CpW(CO)_2$ moieties. However, considersation of the ligand arrangement in **2** suggests that it may also be viewed as an adduct formed between triply bonded $[CpW(CO)_2]_2$ and an "acetylene-like" $Ir_2(CO)_6$ moiety. In particular the structure shows one carbonyl on W(1) which is distinctly nonlinear [W(1)–WC(11)–WO(11) = 167.2 (13)°] and which interacts weakly with W(2)[W(2)–WC(11) = 2.794 (14) Å]. This "semibridging" carbonyl is a characteristic feature displayed in the structures of the acetylene adducts $Cp_2M_2(CO)_4(C_2R_2)$ (M = Mo, R = H, Et, Ph;[13] M = W, R = H[14]), with which the structure of **2** is closely related.

Table I. Butane Hydrogenolysis Data

catalyst type[a]	precursor complex(es)	% ethane[b]	turnover frequency[c]	E_a[d]	H/Ir before[e]	H/Ir after[f]
$[Ir_4]$	$Ir_4(CO)_{12}$	71.0	0.59	45	1.8	1.8
$[WIr_3]$	$CpWIr_3(CO)_{11}$	75.3	5.03	36	1.6	1.4
$[W_2Ir_2]$	$Cp_2W_2Ir_2(CO)_{10}$	49.2	0.86	32	1.5	0.9
$[2W_2 + Ir_4]$	$Cp_2W_2(CO)_6$ + $^1/_2Ir_4(CO)_{12}$	70.4	0.28	48	1.6	1.3

[a] Preparation and pretreatment conditions as described for Figure 3, followed by cooling to 215 °C in H_2. See also ref 28. [b] Percent of ethane in products, the balance being methane and propane. [c] Molecules butane reacted × 10^2 per iridium per s, measured at 215 °C. [d] Apparent activation energy (kcal/mol) over range 200–230 °C. [e] Chemisorption (irreversibly bound H_2) on freshly activated catalysts. [f] Chemisorption on catalysts reheated in H_2 to 500 °C following butane hydrogenolysis.

Compound **2** also is the formal dimer of triply bonded $CpW(CO)_2{\equiv}Ir(CO)_3$ units, which could result from initially formed $CpW(CO)_3Ir(CO)_2NH_2C_6H_4Me$ after loss of the amine and transfer of a carbonyl from tungsten to iridium. Similarly, formation of Ir≡Ir as well as Ir≡W units could lead to the Ir_3W framework of **1**. Indeed, **2** is the stable Ir_2W_2 analogue of the Co_2Mo_2 intermediate proposed by Curtis[15] to explain the products resulting from the reaction $Co_2(CO)_8$ and $Cp_2Mo_2(CO)_4$. There is also a close conceptual analogy to the condensation of $Co_2(CO)_8$ with $CpW(CO)_2{\equiv}CC_6H_4Me$ to form a compound with a pseudotetrahedral Co_2WC core.[16]

In order to prepare catalysts from compounds **1** and **2**, they were absorbed onto γ-alumina[17] from cyclohexane solutions, using air-free techniques similar to those described by Brenner, Burwell, and co-workers.[18] For comparison $Ir_4(CO)_{12}$ and $Cp_2W_2(CO)_6$ were treated similarly. The supported compounds were then decomposed by programmed heating in flowing H_2.[20] Profiles for evolved CO and CH_4 are shown in Figure 3. Our results for $Ir_4(CO)_{12}/Al_2O_3$ are essentially identical with those recently published by Hucul and Brenner[21] and show that most of the coordinated CO is hydrogenated to CH_4 rather than released intact. This feature is true also for the supported bimetallic clusters but to a decreasing extent with an increasing W/Ir ratio; for the W-only material more of the carbonyl ligands are released than reduced. In general there is a trend toward increasing temperatures for methane evolution with increasing tungsten content of the precursor compounds. Significantly, however, the methane profiles for $CpWIr_3(CO)_{11}/Al_2O_3$ and $Cp_2W_2Ir_2(CO)_{10}/Al_2O_3$ are *different*, and neither is the composite of the profiles for $Ir_4(CO)_{12}/Al_2O_3$ and $Cp_2W_2(CO)_6/Al_2O_3$.[22] This indicates that different sites or a different distribution of sites for CH_4 production

---

(7) Spectroscopic data for **1**: ^1H NMR ($CDCl_3$) τ 4.65; IR (ν_{CO}, C_6H_{12}) 2093 s, 2053 vs, 2049 vs, 2031 s, 1996 s, 1979 m, 1967 w.

(8) Spectroscopic data for **2**: ^1H NMR ($CDCl_3$) τ 4.77; IR (ν_{CO}, C_6H_{12}) 2067 s, 2032 vs, 2010 vs, 2000 s, 1987 m, 1968 w, 1926 m, 1896 w, 1833 w.

(9) Crystal data for 1: $C_{16}H_5O_{11}WIr_3$; M = 1133.7; triclinic; space group $P\bar{1}$; a = 8.3137 (16), b = 9.1736 (14), c = 14.1420 (26) Å; α = 91.81 (1), β = 92.86 (2), γ = 103.85 (1)°; U = 1044.9 (3) Å^3; D_c = 3.60 g cm^{-3}; Z = 2; μ(Mo Kα) = 246.4 cm^{-1}. Diffraction data were collected by the θ–2θ scan technique[10] using a Syntex $P2_1$ diffractomer. The structure was solved via conventional Patterson, difference-Fourier, and full-matrix least-squares techniques (anisotropic thermal parameters for metal atoms; isotropic for all other atoms) leading to an R value of 4.8% for all 2737 independent reflections (*none rejected*) with $3 < 2\theta < 45°$. All nonhydrogen atoms were located, and the resulting molecular geometry is shown in Figure 1.

(10) Churchill, M. R.; Lashewycz, R. A.; Rotella, F. J. *Inorg. Chem.* **1977**, *16*, 265.

(11) Crystal data for **2**: $C_{20}H_{10}O_{10}W_2Ir_2$; M = 1162.4; triclinic; space group $P\bar{1}$; a = 8.5028 (24), b = 9.2377 (24), c = 15.6588 (64) Å; α = 87.40 (3), β = 76.61 (3), γ = 73.12 (2)°; U = 1144.7 (5) Å^3; D_c = 3.37 g cm^{-3}, Z = 2, μ(MoKα) = 228.9 cm^{-1}. Diffraction data were collected and treated as described for **1** and the structure was refined to R = 3.6% for the 2998 independent reflections with $3 < 2\theta < 45°$ (*none rejected*). The resulting molecular geometry is shown in Figure 2.

(12) Churchill, M. R.; Hutchinson, J. P. *Inorg. Chem.* **1978**, *17*, 3528.

(13) Bailey, W. I., Jr.; Chisholm, M. H.; Cotton, F. A.; Rankel, L. A. *J. Am. Chem. Soc.* **1978**, *100*, 5764.

(14) Ginley, D. S.; Bock, C. R.; Wrighton, M. S.; Fischer, B.; Tipton, D. L.; Bau, R. *J. Organomet. Chem.* **1978**, 157, 41.

(15) Curtis, M. D.; Klingler, R. J. . *Organomet. Chem.* **1978**, *161*, 23.

(16) Chetucuti, M.; Green, M.; Howard, J. A. K.; Jeffrey, J. C.; Mills, R. N.; Pain, G. N.; Porter, S. J.; Stone, F. G. A.; Wilson, A. A.; Woodward, P. *J. Chem. Soc., Chem. Commun.* **1980**, 1057.

(17) The alumina was Conoco Catapal SB, 60–80 mesh, previously calcined and evacuated at 500 °C, and then cooled to 25 °C under He.

(18) Brenner, A.; Burwell, R. J. *J. Catal.* **1978**, *52*, 353.

(19) Brenner, A.; Hucul, D. A.; Hardwick, S. J. *Inorg. Chem.* **1979**, *18*, 1478.

(20) This procedure has been denoted as TPDE by Brenner.[19]

(21) Hucul, D. L.; Brenner, A. *J. Am. Chem. Soc.* **1981**, *103*, 217.

(22) The profile for $[Ir_4(CO)_{12} + Cp_2W_2(CO)_6]/Al_2O_3$ (W/Ir = 1/1) did appear as the composite of the separate profiles.

are created during the decomposition of the two bimetallic clusters.[23]

The catalytic properties of the materials derived from decomposing the supported clusters have been probed by examining the hydrogenolysis of *n*-butane,[24] the simplest such reaction that offers the possibility of selectivity differences. The resultant data are shown in Table I.[27] The $[Ir_4]$[28] catalyst displayed a high selectivity for scission of the central carbon–carbon bond of butane, forming two molecules of ethane, in agreement with previous studies of highly dispersed Ir/Al_2O_3 catalysts, specifically Anderson's study using $Ir_4(CO)_{12}$ as a precursor.[29] The $[WIr_3]$[28] and $[2W_2 + Ir_4]$[28] catalysts also showed ethane selectivity of 70% or greater, but the $[W_2Ir_2]$[28] catalyst showed less than 50% ethane in the product stream. This substantially different cracking pattern for the $Cp_2W_2Ir_2(CO)_{10}$-derived catalyst is strong evidence for a residual tungsten–iridium interaction that modifies the character of the catalytic site(s). The activities measured were comparable with previous data for Ir/Al_2O_3,[29] but most noteworthy is that the activation energies were lower for both the $[WIr_3]$ and the $[W_2Ir_2]$ catalysts.

Chemisorption data have been collected as partial physical characterization of the cluster-derived catalysts.[30] Freshly activated materials showed irreversibly adsorbed quantities of H_2 and CO corresponding to H/Ir = 1.5–1.8 and CO/Ir = 1.0–1.3. These values indicate very high dispersions, with particle sizes probably less than 10 Å.[31] The mixed-metal catalysts showed some loss of metal surface area after the hydrogenolysis experiments. However, electron microscopy studies revealed no discernable particles under conditions where ≥20-Å particles were seen in conventionally prepared catalyst samples. The diminished chemisorption was particularly true of the $[W_2Ir_2]$ catalyst and may indicate the formation of carbonaceous residues during the catalytic runs.

Further physical as well as catalytic studies are being conducted with the bimetallic cluster-derived catalysts. Nevertheless, the present work shows that the synthetic and structural methodology of inorganic chemistry can provide suitable precursors to bimetallic catalysts, combining rather disparate elements. More significantly, it indicates that the catalytic properties derived may be uniquely linked to the specific bimetallic precursor.[32] This result offers the possibility of enhanced control and even the effective design of bimetallic catalytic sites.

Acknowledgment. This research was supported at the University of Illinois by NSF Grants DMR 77-23999 and 80-20250 and at SUNY-Buffalo by NSF Grant CHE 80-23448. J.R.S. is grateful for the interest shown in this work by Dr. John Sinfelt and acknowledges very helpful discussions with him, Dr. Gary McVicker, and Al Barnett.

Supplementary Material Available: Lists of positional and thermal parameters (4 pages). Ordering information is given on any current masthead page.

---

[23] Cp ligands of the mixed metal clusters were hydrogenated and cracked above 300 °C. However, quantitative data indicate an upper limit of 10% of the CH_4 produced can be due to Cp cracking.

[24] Catalytic activity for *n*-butane hydrogenolysis was monitored by gas chromatography. Conversions were kept less than 5% to eliminate complications due to heat and mass transfer. Catalytic activities at different temperatures were bracketed by runs at standard conditions to minimize possible effects of catalyst deactivation.[25,26] Both activities and product distributions showed good reproducibility at any given temperature and neither varied appreciably with time or after reactivation. A 150-cc/min flow rate, 20:1 H_2–*n*-butane, was employed.

[25] Yates, D. J. C.; Taylor, W. F.; Sinfelt, J. H. *J. Am. Chem. Soc.* **1964**, *86*, 2996.

[26] Vannice, M. A. *J. Catal.* **1975**, *37*, 449.

[27] Neither the decomposed $Cp_2W_2(CO)_6/Al_2O_3$ nor the Al_2O_3 alone was active in the temperature range used (<230 °C).

[28] This abbreviation is meant only to indicate the precursor to the supported metal species, with no implications regarding the actual particle size, shape, or composition.

[29] Foger, K.; Anderson, J. R. *J. Catal.* **1979**, *59*, 325.

[30] Hydrogen and carbon monoxide chemisorption were measured volumetrically by using conventional procedures.[31]

[31] G. B. McVicker, Baker, R. T. K.; Garten, R. L.; Kugler, E. L. *J. Catal.* **1980**, *65*, 207.

[32] Two reports have indicated finding no evidence for bimetallic interactions influencing the activity of cluster-derived catalysts: (a) Thomas, T. J.; Mistalski, G.; Hucul, D. A.; Brenner, A. 179th National Meeting of the American Chemical Society, Houston, TX, March 1980; American Chemical Society: Washington, DC, 1980; Abstr. COLL 11. (b) Shapley, J. R.; Hardwick, S. J.; Foose, D. S.; Stucky, G. D. *Prepr., Div. Pet. Chem., Am. Chem. Soc.* **1980**, *25*, 780. However, for contrary indications, see: (c) McVicker, G. B. U.S. Patent 4 187 168, 1980.

Remarkably Facile Os–Os Bond Cleavage in the Reaction of $H_2Os_3(CO)_{10}$ with a Tungsten Carbyne. Crystal Structures of $CpWOs_3(CO)_{11}[C(O)CH_2C_6H_4Me]$ and $Cp_2W_2Os(CO)_7[C_2(C_6H_4Me)_2]$

John R. Shapley* and Joon T. Park

Department of Chemistry and
Materials Research Laboratory
University of Illinois, Urbana, Illinois 61801

Melvyn Rowen Churchill,* Clifford Bueno, and
Harvey J. Wasserman

Department of Chemistry
State University of New York at Buffalo
Buffalo, New York 14214

Received August 10, 1981

Stone and co-workers have utilized the "isolobal" analogy between an alkyne ($RC{\equiv}CR$) and a metal carbyne complex ($L_nM{\equiv}CR$)[1] as motivation for examining the interaction of a variety of reactive low oxidation state compounds with metal carbynes.[2] Intrigued by the success of this analogy, we decided to examine it in the particular instance of $H_2Os_3(CO)_{10}$, which cleanly inserts many alkynes to form the alkenyl derivatives $HOs_3(CO)_{10}(CR{=}CHR)$.[3] We wish to report that $H_2Os_3(CO)_{10}$ indeed reacts easily with a typical carbyne complex, but by two parallel reaction paths, only one of which involves hydrogen transfer. In contrast to the reaction with alkynes, however, both paths involve cleavage of Os–Os bonds under very mild conditions.

A cold (−30 °C) dry dichloromethane solution of $Cp(CO)_2W{\equiv}CC_6H_4Me$ (90 mg, 0.22 mmol) was added to a dry dichloromethane solution of $H_2Os_3(CO)_{10}$ (195 mg, 0.23 mmol) at 0 °C. The reaction mixture was stirred at 0 °C for 5 h and then warmed to room temperature. Evaporation of the solvent and preparative TLC (silica gel/3:2 dichloromethane–pentane) provided the two major products,[4] dark red $CpWOs_3(CO)_{12}(CH_2C_6H_4Me)$ (**1**, 59 mg, 21%) and red $Cp_2W_2Os(CO)_7(CC_6H_4Me)_2$ (**2**, 40 mg, 33%), isolated as crystalline solids. These formulations were established by spectroscopic and analytical data,[5] but a reasonable structure could be formulated only for compound **2**. The actual structures of both **1** and **2** have been

---

[1] Ashworth, T. V.; Howard, J. A. K.; Stone, F. G. A. *J. Chem. Soc., Chem. Commun.* **1979**, 42.

[2] Ashworth, T. V.; Chetcuti, M. J.; Howard, J. A. K.; Stone, F. G. A.; Wisbey, S. J.; Woodward, P. *J. Chem. Soc., Dalton Trans.* **1981**, 763 and references therein.

[3] Clauss, A. D.; Tachikawa, M.; Shapley, J. R.; Pierpont, C. G. *Inorg. Chem.* **1981**, *20*, 1528 and references therein.

[4] A third, minor product has been isolated and characterized spectroscopically and structurally as $CpWOs_3(CO)_{10}(CAr)_2H$. Formation of this compound involves cleavage of a $W{\equiv}C$ bond as well as an Os–Os bond. Details are still under investigation and will be reported in a full paper.

[5] Compound **1**: IR (CCl_4) $\nu(CO)$ 2095 (m), 2063 (vs), 2032 (m), 2021 (s), 2007 (m), 1978 (m), 1939 (vw) cm^{-1}; ^1H NMR (CD_2Cl_2, 25 °C) δ 7.15–7.20 (m, 4 H), 5.43 (s, 5 H), 3.47 (s, 2 H), 2.35 (s, 3 H); mass spectrum (70 eV, ^{192}Os, ^{184}W), m/z 1266 (M^+). Anal. Calcd for $C_{25}H_{14}O_{12}WOs_3$: C, 23.82; H, 1.12; W, 14.58; Os, 45.26. Found: C, 24.18; H, 1.21; W, 14.53; Os, 42.64. Compound **2**: IR (CCl_4)$\nu(CO)$ 2061 (w), 2046 (vs), 1998 (sh), 1990 (vs), 1977 (vs), 1959 (sh), 1918 (s), 1830 (w) cm^{-1}; ^1H NMR (CD_2Cl_2, 25 °C) δ 6.9–6.7 (m, 8 H), 5.06 (s, 10 H), 2.23 (s, 6 H); mass spectrum (field desorption, ^{192}Os, ^{184}W), m/z 1092 (M^+). Anal. Calcd for $C_{33}H_{24}O_7W_2Os$: C, 36.35; H, 2.22; W, 33.72; Os, 17.44. Found: C, 36.17; H, 2.17; W, 33.20; Os, 16.00.

0002-7863/81/1503-7385$01.25/0